



Published in final edited form as:

Mutat Res. 2015 September ; 779: 86–95. doi:10.1016/j.mrfmmm.2015.06.011.

Environmental and chemotherapeutic agents induce breakage at genes involved in leukemia-causing gene rearrangements in human hematopoietic stem/progenitor cells

Ryan G. Thys^{a,1}, Christine E. Lehman^{a,1}, Levi C.T. Pierce^b, and Yuh-Hwa Wang^c

Ryan G. Thys: rthys@wakehealth.edu; Christine E. Lehman: clehman@wakehealth.edu; Levi C.T. Pierce: Levipierce@gmail.com; Yuh-Hwa Wang: yw4b@virginia.edu

a

b

c

Abstract

Hematopoietic stem and progenitor cells (HSPCs) give rise to all of the cells that make up the hematopoietic system in the human body, making their stability and resilience especially important. Damage to these cells can severely impact cell development and has the potential to cause diseases, such as leukemia. Leukemia-causing chromosomal rearrangements have largely been studied in the context of radiation exposure and are formed by a multi-step process, including an initial DNA breakage and fusion of the free DNA ends. However, the mechanism for DNA breakage in patients without previous radiation exposure is unclear. Here, we investigate the role of non-cytotoxic levels of environmental factors, benzene, and diethylnitrosamine (DEN), and chemotherapeutic agents, etoposide, and doxorubicin, in generating DNA breakage at the patient breakpoint hotspots of the *MLL* and *CBFB* genes in human HSPCs. These conditions represent exposure to chemicals encountered daily or residual doses from chemotherapeutic drugs. Exposure of HSPCs to non-cytotoxic levels of environmental chemicals or chemotherapeutic agents causes DNA breakage at preferential sites in the human genome, including the leukemia-related genes *MLL* and *CBFB*. Though benzene, etoposide, and doxorubicin have previously been linked to leukemia formation, this is the first study to demonstrate a role for DEN in the generation of DNA breakage at leukemia-specific sites. These chemical-induced DNA breakpoints coincide with sites of predicted topoisomerase II cleavage. The distribution of breakpoints by exposure to non-cytotoxic levels of chemicals showed a similar pattern to fusion breakpoints in leukemia patients. Our findings demonstrate that HSPCs exposed to non-cytotoxic levels of environmental chemicals and chemotherapeutic agents are prone to topoisomerase II-mediated DNA damage at the leukemia-associated genes *MLL* and *CBFB*. These data suggest a role for long-term environmental chemical or residual chemotherapeutic drug exposure in generation of DNA breakage at sites with a propensity to form leukemia-causing gene rearrangements.

This is an open access article under the CC BY-NC-ND license (<http://creativecommons.org/licenses/by-nc-nd/4.0/>).

Correspondence to: Yuh-Hwa Wang, yw4b@virginia.edu.

¹These authors contributed equally to this work.

Conflict of interest

The authors declare that there is no conflict of interest.

Keywords

CBFB; Fragile site; Hematopoietic stem cells; Leukemia; MLL; Topoisomerase II

1. Introduction

Leukemia is one of the leading causes of male and female cancer deaths in the United States. Most leukemias are thought to originate in hematopoietic stem or progenitor cells and are typically associated with a variety of genetic alterations, including gene rearrangements or copy number variations [1]. The formation of gene rearrangements that cause leukemia is a multi-step process, including the initial double-stranded DNA breakage and subsequent joining together of the gene pairs. Ionizing radiation has been shown to cause rearrangement-generating DNA breakage, but in patients without previous exposure to radiation, the mechanism is unknown. However, exposure to a number of environmental chemicals and chemotherapeutic agents has been linked to development of leukemia, making it one of the most common types of cancer induced by a variety of cancer-causing agents [1]. Interestingly, many of these same chemicals, including benzene, induce the expression of chromosomal fragile sites, suggesting a potential mechanism for generation of DNA breakage that leads to gene rearrangement [2]. While the two chemotherapeutic drugs etoposide and doxorubicin have not previously been linked directly to fragile site breakage, inhibition of their therapeutic target, DNA topoisomerase II, has been suggested to play a role in fragile site instability [3].

Chromosomal fragile sites are regions of the genome susceptible to breakage under conditions of replication stress. Fragile site breakage is typically induced in the laboratory by treatment of cells with low doses of the DNA polymerase inhibitor, aphidicolin (APH). Low-dose APH exposure leads to expression of over 230 fragile sites in human cells [4]. In addition to APH, fragile sites are prone to break following exposure to many chemicals, including environmental and chemotherapeutic agents (reviewed in [5]). Therefore, understanding both the mechanism for, and consequences of, fragile site breakage following exposure to such chemicals will be important in guiding treatment decisions and preventing exposures that may cause human disease.

Fragile site breakage is associated with a number of human diseases, including cancer. Many gene rearrangements and copy number variations in cancer occur at genes located within fragile sites [6,7]. The most frequently expressed fragile site, FRA3B, is located within the tumor suppressor *FHIT*, and exposure of cells to APH induces submicroscopic deletions within *FHIT* that are consistent with those seen in numerous cancers, including esophageal, breast, and small-cell and non-small cell lung carcinomas [8]. Furthermore, exposure of human thyroid cells to fragile site-inducing conditions leads to formation of the *RET/PTC* rearrangement that causes papillary thyroid carcinoma [9]. In addition to the *RET/PTC* rearrangement in papillary thyroid carcinoma, over half of cancer-causing gene rearrangements contain at least one gene located within a fragile site [10]. A large number of these rearrangements are associated with various leukemias, such as acute myeloid leukemia and acute lymphoblastoid leukemia, suggesting a role for fragile site breakage in leukemogenesis. Two leukemia-associated genes located within fragile sites are *MLL*,

located within FRA11G, and *CBFB*, located within FRA16C. DNA breakage within *MLL* can lead to rearrangement with over 120 partner genes, resulting in acute leukemias with typically poor prognosis [11]. *MLL* rearrangements are found in approximately 10% of leukemias [12] and 25% of therapy-related AML [13]. Mapping of patient breakpoints has identified a breakpoint cluster region (BCR) spanning exons 8–12, with *de novo* breakpoints within a 3-kb region between exons 9 and 11, and therapy-related leukemia breakpoints clustering at the intron 11/exon 12 junction [11,14]. DNA breakage within *CBFB* can lead to the *inv(16)* and related *t(16;16)(p13;q22)* rearrangement found in approximately 10% of all *de novo* acute myeloid leukemias. All *CBFB* breakpoints involved in these rearrangements have been mapped to intron 5, and all are associated with the M4Eo subtype [15,16]. Many studies have demonstrated that rearrangement formation within hematopoietic stem and progenitor cells (HSPCs) can promote the formation of leukemia [17–20]; however, the role of fragile site breakage in the generation of these rearrangements has yet to be investigated.

HSPCs are the cells from which all cells of the hematopoietic system are derived [1]. These cells are capable of self-renewal and differentiation into mature blood cells found throughout the body. While HSPCs are typically found in the bone marrow, they are able to move throughout the peripheral blood to a number of tissues at low levels, and also are released in larger numbers in response to cytokines, growth factors, and under conditions of stress or myelosuppression [21–23]. The mobility of these cells throughout the body may leave them susceptible to exposure to DNA damaging agents, such as environmental chemicals or chemotherapeutic agents, which have the potential to lead to leukemogenesis.

The location of leukemia-associated genes within common fragile sites and the role of environmental chemicals and chemotherapeutic agents in fragile site instability, leukemogenesis, and topoisomerase interaction prompted us to investigate whether these compounds cause DNA breakage at leukemia-associated fragile sites. The sensitivity of the BCRs of *MLL* and *CBFB* to the environmental chemicals, benzene, and diethylnitrosamine (DEN), or the chemotherapeutic agents, etoposide, and doxorubicin, in human CD34⁺ HSPCs was determined by ligation-mediated PCR (LM-PCR). The nucleotide positions of chemical-induced breakpoints were mapped to sites of topoisomerase II cleavage, using DNA secondary structure predictions and sequence analysis. The distribution of chemical-induced breakpoints in our studies was compared to that of fusion breakpoints found in leukemia patients. The results suggest a role for topoisomerase II in breakage at leukemia-associated fragile sites in human CD34⁺ HSPCs in response to chemical agents linked to leukemogenesis, such as benzene, etoposide and doxorubicin, and also DEN, which has not been previously connected to leukemogenesis.

2. Materials and methods

2.1. Cells and culture conditions

Experiments were performed using primary human CD34⁺ bone marrow stem and progenitor cells (ALLCELLS), grown in Hematopoietic Growth Medium (Lonza) supplemented with StemSpan CC100 (StemCell Technologies) containing IL-3, IL-6, Stem Cell Factor and FLT-3 ligand.

2.2. Cell treatments and analyses

To analyze cell viability, human CD34⁺ cells (1×10^5) were plated in 12-well plates and treated immediately with chemical concentrations as indicated in the text for 24 h. Cells were collected, washed with phosphate-buffered saline (PBS; Invitrogen), and re-suspended in PBS containing 2 µg/mL propidium iodide. Cell viability was determined using a Becton Dickinson FACSCalibur flow cytometer (BD Biosciences). Various concentrations of benzene (0.5–1 mg/mL), diethylnitrosamine (DEN, 1.5–3.0 mg/mL), etoposide (150 nM–10 µM), and doxorubicin (5–700 nM) were examined to determine the optimal dosage for the treatment of CD34⁺ cells.

To analyze active apoptosis, CD34⁺ cells (1×10^5) were plated and treated as above for 24 h. Cells were then washed with PBS and re-suspended in 1X annexin V binding buffer. Annexin V (BD Biosciences) was then added to each sample and incubated in the dark for 15 min. Early apoptotic cells were quantified using a FACSCalibur flow cytometer.

To analyze cell growth, viable CD34⁺ cells (0.65×10^5) were determined by trypan blue exclusion using a hemocytometer, plated, and treated in 12-well plates. Cells were harvested after 24 h, washed with PBS, and re-plated with fresh media. Cells were again quantified while re-plating and after they had been allowed to recover for an additional 24 h in chemical-free media.

To analyze cell cycle progression, CD34⁺ cells (5×10^5) were plated and treated with the chemical concentrations indicated in the text for 24 h. Following treatment, cells were collected, washed with PBS and fixed in ethanol. Cells were then resuspended in PBS containing RNase and propidium iodide for 20 min in the dark. Subsequently, the cells were analyzed using a FACSCalibur flow cytometer to determine DNA content.

2.3. DNA breakpoint detection by LM-PCR

To detect DNA breaks, genomic DNA was isolated from human CD34⁺ progenitor cells following treatment for 24 h and compared with untreated cells. Blunt-ended double-stranded DNA breaks were detected and quantified as described previously [9], with modifications as follows. Genomic DNA was directly ligated to the asymmetrical duplex LL3/LP2 linker, and ligation mixtures were then purified through Sephadex G-100 columns prior to nested PCR. To amplify the ligated DNA breaks, linker-specific primers LL4 and LL2 were used in combination with region-specific primers in the first and second rounds of nested PCR, respectively (Supplemental Table 3). The final PCR products were then resolved by gel electrophoresis and sequenced to identify the breakpoint location adjacent to the LL3/LP2 linker sequence.

2.4. DNA secondary structure prediction

DNA secondary structure formation was determined using the Mfold program [24], which predicts and assigns free energy values based on the potential of single-stranded DNA to form stable secondary structures. Segments of 300-nt were analyzed sequentially with a 150-nt shift along a 15.7 kb region (chr11: 118,348,501-118,364,250) spanning the *MLL* BCR or the entire chromosome 11 (human genome build 37.2). The most stable predicted secondary

structure was used to analyze the location of chemical-induced DNA breaks within the patient BCR of *MLL*.

2.5. Chemical breakpoint mapping to topoisomerase II cleavage sites

Chemical-induced breakpoints were determined by Sanger sequencing following LM-PCR. The breakpoints were then mapped to topoisomerase II cleavage sites based on preferential cleavage on consensus sequences or predicted DNA secondary structures. The consensus sequences are [5'-(no A) (no T) (A/no C) (-) (C/no A) (-)(-) (-) (-) (no T) (-) (T/no G) (C/no A) (-)-3'], where breakage occurs between nucleotides five and six [25], and the consensus sequence [5'-(A) (T) (T) (A/T)- 3'], where the breakage occurs before the first nucleotide [26]. DNA secondary structures of each region were predicted using the Mfold program to analyze the DNA sequence spanning from 50-bp upstream to 1000-bp downstream of the second round PCR primer in 300-nt segments with sequential shifts of 150-nt. Topoisomerase II cleaves DNA hairpins one nucleotide from the junction of the 3'-base of a hairpin stem with single-stranded DNA [27], and also cleaves within the single-stranded DNA loop of the hairpin structure [28]. We applied these criteria to determine the cleavage sites on the structure with the most favorable free energy value.

2.6. Statistical analysis

p-Values were calculated using two-tailed Student's *t*-tests. Multiple comparisons analysis was performed using a single-factor ANOVA followed by Bonferonni correction.

3. Results

3.1. The classic fragile site-inducing chemical, APH, causes DNA breakage at the BCR of genes involved in leukemia-associated gene rearrangements

Because the location of the leukemia-associated genes *MLL* and *CBFB* are mapped to known fragile sites, we examined whether low-dose APH (a classic fragile site-inducing condition) induces DNA breaks within the BCRs of *MLL* and *CBFB* in human CD34⁺ HSPCs derived from the bone marrow of healthy donors. To determine DNA break frequency within the BCRs of *MLL* (exons 8–12) [11], and *CBFB* (intron 5) [16], HSPCs were treated with 0.4 μM APH for 24 h, and the genomic DNAs from both the treated and untreated cells were subjected to LM-PCR, by ligating to a linker. The linker-attached DNAs were isolated, amplified by two rounds of nested PCR, visualized by agarose gel electrophoresis (Fig. 1A and Supplemental Fig. 1), and sequenced to locate the breakpoints. Each lane on the gel represents the DNA breaks from approximately 1300 cells, and each band observed on the gel corresponds to a break found within the region of interest. Three regions within the BCR of *MLL* were examined (*MLL* i9, *MLL* i10, *MLL* e12; Fig. 4). Treatment of HSPCs with low-dose APH induced significantly higher DNA breakage within the BCRs of *MLL* and *CBFB*, compared to those in the untreated cells (Fig. 1B). The intron 9 (*MLL* i9) and intron 10 (*MLL* i10) regions, both of which are located within the *de novo* leukemia patient breakpoint clusters, displayed significant sensitivity to APH in HSPCs. Investigation of the intron 11/exon 12 junction (*MLL* e12), the cluster site of the therapy-related leukemia breakpoints, found that while APH induces DNA breakage at this site, the overall amount of breakage within this region is higher than all other regions studied, even

without APH treatment, suggesting an inherent fragility at this site. Breakage within intron 5 of *CBFB* (*CBFB* i5) following APH treatment was significantly higher than in untreated cells. The *FHIT* gene encompassing fragile site FRA3B, the most fragile site in the genome [29], also showed a significant increase in breakage upon APH treatment, while non-fragile regions at chromosome 12p12.3 and *G6PD* [30] were insensitive to fragile site induction. These results demonstrate that the exposure of HSPCs to APH induces the formation of DNA breaks within the BCRs of both *MLL* and *CBFB*, and these regions are therefore within bona fide fragile sites in HSPCs.

Intron 11 of the *RET* gene, located within fragile site FRA10G and involved in the thyroid cancer-causing *RET/PTC* rearrangement [31], is also sensitive to APH in HSPCs (Fig. 1B). However, overall breakage within *RET* occurred at a much lower level than at *MLL* or *CBFB* in HSPCs ($p < 0.01$), suggesting a molecular basis for occurrence of leukemia-causing gene rearrangements, with leukemia-associated genes showing an increased susceptibility to breakage compared to non-leukemia-associated genes.

3.2. Environmental chemicals and chemotherapeutic drugs induce DNA breakage in BCRs of *MLL* and *CBFB* in human CD34⁺ HSPCs

Many fragile site-inducing environmental chemicals are encountered daily, including benzene, found in cigarette smoke and gasoline fumes, and DEN, found in cigarette smoke, pesticides, and foods such as cured meats [2]. Interestingly, exposure to benzene is strongly linked to leukemia formation [1].

Here, optimal dosages of benzene and DEN for the 24 h treatment of HSPCs were first determined by cell viability assay (Fig. 2A), such that significant levels of cell death were not induced, in order to mimic daily low level exposure to environmental chemicals. Treatment of HSPCs with 0.5 mg/mL benzene or 1.5 mg/mL DEN did not induce apoptosis, as measured by flow cytometric analysis of annexin V staining (Fig. 2B). Cell growth, measured by trypan blue exclusion, was not perturbed following treatment with benzene but showed a delay upon DEN treatment (Fig. 2C). Further, treatment of HSPCs with benzene or DEN did not perturb cell cycle progression (Supplemental Fig. 2).

To investigate whether exposure of HSPCs to non-cytotoxic levels of benzene and DEN can cause DNA breakage at the leukemia-related genes *MLL* and *CBFB*, HSPCs were treated with 0.5 mg/mL benzene or 1.5 mg/mL DEN for 24 h, and breakage within the BCRs of *MLL* and *CBFB* was analyzed by LM-PCR. In the *MLL* and *CBFB* BCRs, both benzene- and DEN-induced breakage was significantly higher than in untreated cells (Fig. 3). The frequencies of DNA breakage induced by benzene or DEN in the BCRs of *MLL* and *CBFB* were similar to that of APH-induced breakage, as *MLL* e12 was the most fragile site. Interestingly, benzene and DEN induced different amounts of breakage across the sites within *MLL* and *CBFB*, suggesting that diverse *cis* and/or *trans* factors are responsible for breakage at each site.

The *RET* region had a similar, significant increase in DNA breakage following exposure to benzene and DEN, though at significantly lower levels than *MLL* and *CBFB* ($p < 0.01$). The 12p12.3 non-fragile region was insensitive to benzene; however, DEN caused a significant

increase in breakage. Another non-fragile region, *G6PD*, was not susceptible to significant breakage by either chemical. These results demonstrate the sensitivity of leukemia-associated fragile sites in HSPCs to benzene exposure, suggesting a role for environmental factors in generation of DNA breakage at leukemia-causing genes through a fragile site-mediated mechanism. While DEN exposure caused an increase in breakage at *MLL* and *CBFB*, the non-fragile 12p12.3 region was also sensitive to the treatment, but the *G6PD* region was not. Therefore, the breakage from DEN-induced exposure is not limited to fragile sites, and perhaps other factors contribute to the sensitivity of the 12p12.3 region.

Treatment of primary tumors with chemotherapy regimens containing etoposide or doxorubicin are linked to formation of secondary, or therapy-related, leukemias [1]. While several chemotherapeutic agents are known to cause breakage at fragile sites [32], etoposide, and doxorubicin have not previously been studied in this regard. Using pharmacokinetic studies as a guide to mimic residual dose from chemotherapy administration [33,34], we treated HSPCs with various concentrations of etoposide or doxorubicin for 24 h. Fig. 2A–C show that 0.15 μM etoposide or 5 nM doxorubicin did not induce cell death, and cell growth was not affected.

Next, we examined DNA breakage resulting from exposure of HSPCs to 0.15 μM etoposide or 5 nM doxorubicin for 24 h, and found that these low doses of drugs caused significant breakage at introns 9, and exon 12 of *MLL*, as well as intron 5 of *CBFB*, relative to untreated cells. The exon 12 region of *MLL* is linked to topoisomerase II-dependent breakage, due to the presence of a putative topoisomerase II recognition motif [14,35–37]. Therefore, the high level of breakage induced by etoposide, a topoisomerase II inhibitor, reflects the sensitivity at this site and confirms the involvement of DNA topoisomerase II. More importantly, the concentration of etoposide used in our studies is 100–1000-fold lower than in previous *in vitro* studies [35,37] and about 300–1000-fold lower than in the plasma of patients immediately after receiving treatment [33,34]. These results suggest that cells able to survive chemotherapy regimens are still susceptible to DNA breakage in leukemia-associated genes when exposed to a residual dose of the treatment. While many of the cells exposed to chemotherapeutic drugs at doses typically used in therapy are killed, cells in circulation that are not killed are at risk of adverse effects due to exposure to low-dose and non-cytotoxic levels of these drugs.

Interestingly, 12p12.3 is susceptible to breakage caused by etoposide and doxorubicin treatments, while *RET* and *G6PD* are not. Using DNA topoisomerase II consensus sequences of recognition/cleavage [25,26], we determined the number of predicted topoisomerase II sites within the DNA sequence (1050-bp each) of all regions probed by LM-PCR. The 1050-bp regions extended 50-bp upstream and 1000-bp downstream from the second round region-specific primer for each region and represent the region analyzed in our DNA breakage studies. We found that within all *MLL* and *CBFB* regions, a range of 33–48 predicted topoisomerase II consensus sites were present in the sequences, and the *FRA3B* sequence contained 36 consensus sites (Supplemental Table 1). Notably, the *RET* and *G6PD* sequences had only 15 and 11 predicted topoisomerase II consensus sites, respectively, while the 12p12.3 region contained 67 topoisomerase II sites, more than all other regions analyzed. The number of topoisomerase II consensus sites could help to explain both the

sensitivity of the 12p12.3 region and the insensitivity of the *RET* and *G6PD* regions to both etoposide and doxorubicin in HSPCs, as the presence of more topoisomerase II consensus sites leads to more DNA breakage upon treatment. These results further indicate a critical role for DNA topoisomerase II in promoting DNA breakage at leukemia-associated genes in HSPCs.

3.3. The patient BCRs of *MLL* are predicted to form stable DNA secondary structures

Stable DNA secondary structure has been suggested to contribute to fragile site breakage [32,38], and it serves as a determinant for DNA topoisomerase II recognition and cleavage [27,28]. To investigate whether DNA secondary structure is responsible for DNA breakage in the BCR of *MLL*, the Mfold program was used to predict the ability of the *MLL* BCR to form stable DNA secondary structure [24]. We analyzed 300-nucleotide segments with a 150-nucleotide shift and determined the most stable structures for each segment along a 15.7-kb sequence from exon 6-intron 17 (chr11: 118348501-118364250), which includes the *MLL* BCR (exons 8 to 12, chr11: 118352430-118359475) (Fig. 4). Within the 7 kb *MLL* BCR derived from mapping leukemia patient breakpoints, the sites are not evenly distributed, with *de novo* breakpoints occurring throughout a 3 kb region between exons 8 and 11, and therapy-related leukemia breakpoints clustering at the intron 11/exon 12 junction [11]. Approximately, half of the segments (24/49) within the *MLL* BCR were predicted to form stable secondary structures, as their free energy of structure formation was lower than the average free energy for chromosome 11. Six out of 49 segments had a predicted free energy of structure formation within the most stable 10% of all segments along chromosome 11. These structure-forming sites are located in regions that were identified as hotspots for breakage in both *de novo* and therapy-related leukemia [11], with four segments located within the *de novo* breakpoint cluster and two in the therapy-related breakpoint cluster. These results suggest that DNA secondary structure could influence DNA breakage formation in the patient breakpoint hotspots of *MLL*.

3.4. Environmental chemical- and chemotherapeutic-induced breakpoints are located at predicted DNA topoisomerase II cleavage sites

In addition to the recognition of consensus sequences in double-stranded DNA, DNA topoisomerase II recognizes and preferentially cleaves single-stranded DNA within regions that form DNA secondary structures [3,27,28,35]. DNA topoisomerase II cleaves DNA hairpins one nucleotide from the 3'-base of the stem, where DNA secondary structure and the presence of a double-stranded/single-stranded DNA junction at the 3'-base of the hairpin, rather than sequence specificity, are the predominant features recognized by the enzyme [27]. Additionally, human topoisomerase II α recognizes hairpin structures formed within alpha satellite DNA and cleaves within the single-stranded DNA loop region of the hairpin structure [28]. Using these structural criteria combined with the consensus sequences, the locations of the etoposide-induced breakpoints were first compared with the locations of the predicted topoisomerase II cleavage sites in two *MLL* regions (*MLL* i9 and *MLL* e12) and the *CBFB* (*CBFB* i5) region. Because etoposide specifically interacts with topoisomerase II to inhibit its re-ligation activity, etoposide-induced breakpoints allowed us to verify that topoisomerase II cleaves DNA within these regions, and that these cleavage sites correspond to the predicted sites generated from considering both consensus sequences

and associated DNA secondary structure features. A total of 55 etoposide-induced breakpoints located in MLL i9, MLL e12, and CBF*B* i5 regions were analyzed. We found that 88%, 95%, and 100% of etoposide-induced breakpoints corresponded to predicted topoisomerase II cleavage sites in MLL i9, MLL e12, and CBF*B* i5 regions, respectively (Table 1), with the remaining breakpoints in MLL i9 and MLL e12 located within three nucleotides of the predicted cleavage sites. These results verify the involvement of topoisomerase II in generation of DNA breakage within the breakpoint cluster regions of *MLL* and *CBF*B** and indicate the utility of the predicted cleavage sites. For 59 doxorubicin-induced breakpoints, 90%, 90%, and 83% corresponded to predicted topoisomerase II cleavage sites in MLL i9, MLL e12, and CBF*B* i5 regions, respectively, and greater than 93% were located within one nucleotide of predicted topoisomerase II cleavage sites, further supporting the role of topoisomerase II in DNA breakage at these regions.

The percentage of benzene and DEN-induced breakpoints mapped to predicted topoisomerase II cleavage sites in the MLL e12 (96% and 97%, respectively) and CBF*B* i5 (95% and 90%, respectively) regions indicates a strong influence of topoisomerase II on break formation in these regions, compared to those in the MLL i9 region (78% and 64%, respectively). In these three regions, while the significantly low frequency of DNA breaks was observed in untreated cells compared to those of all treatments (Fig. 3), the frequencies of breaks at topoisomerase sites by all treatments were significantly higher than in untreated cells ($p < 0.05$) with the exception of benzene-treated MLL i9 region (Table 1, last column). Within the MLL e12 region, 51 of the 120 breakpoints induced by a combination of all treatments occurred within an 11-nt sequence (chr11: 118359356-118359366) containing a previously identified topoisomerase II cleavage site [14,36,37]. Twenty-three of the fifty-one breaks at this site were induced by benzene and DEN, representing 48% of the total benzene and DEN-induced sites in the MLL e12 region. While the etoposide- and doxorubicin-induced breakpoints were expected to map to the topoisomerase II sites, the overlap of benzene and DEN-induced break sites with topoisomerase II sites in MLL e12 suggests an involvement of DNA topoisomerase II in break formation caused by benzene or DEN exposure. Benzene and its metabolites have been shown to interact with topoisomerase II [30,39], but DEN has not been linked to topoisomerase II. Our findings that 97% of DEN-induced breaks correspond to topoisomerase II cleavage sites in the intron 11/exon 12 junction of *MLL* are the first to suggest a link between DEN and topoisomerase II-mediated DNA breakage.

3.5. Distribution of environmental chemical- and chemotherapeutic-induced breakpoints resemble those of fusion breakpoints in leukemia patients

While the chemical-induced breakpoints in our study were determined before a translocation event, the locations of breakpoints identified in leukemia patients are identified following rearrangement. Therefore, to investigate the relationship between the chemical-induced breakpoints and subsequent rearrangement processes, we compared the locations of the chemical-induced breakpoints with the locations of breakpoints identified in leukemia patients containing known *MLL* rearrangements [11]. Meyer et al., carried out a comprehensive study of leukemia patients with *MLL* rearrangements and revealed patient breakpoints concentrated in the BCR with an uneven distribution [11], which we clearly

demonstrated in the *MLL* i9 and *MLL* e12 regions (Fig. 5). The patient breakpoints were located uniformly throughout the *MLL* i9 region, while a peaked pattern of distribution was observed in the *MLL* e12 region. Upon analyzing 110 and 120 chemical-induced breakpoints of the *MLL* i9 and *MLL* e12 regions, respectively, we found a striking similarity in the distribution patterns when compared to patient fusion breakpoints. Within the *MLL* i9 region, no hotspots of chemical-induced cleavage were present, as seen among the patient fusion breakpoints. Interestingly, chemical-induced cleavage in the *MLL* e12 region showed a peaked distribution similar to that of patient fusion breakpoints but with the hotspot shifted about 250 bp downstream, suggesting a subsequent nuclease degradation process after initial cleavage and prior to the fusion event. Analysis of reciprocal fusions in patients supports this notion by showing that in most leukemia fusions, deletions are observed surrounding the fusion points, with 52% ranging from 1 to 50 bp, 38% from 51 to 600 bp, and 10% from 700 bp to 4.4 kb [11]. These data suggest that exposure of *MLL* to environmental chemicals or chemotherapeutic agents, such as those investigated in our study, lead to double-stranded DNA breakage with the potential to form leukemia-causing gene rearrangements corresponding to those seen in patients. Rearrangement formation at these sites occurs through a mechanism in which processing of the free ends of broken DNA can result in the loss of up to 4 kb of genomic material. Further investigation of the effects of long-term exposure to low doses of environmental and chemotherapeutic agents as well as their role in leukemogenesis appears to be warranted.

4. Discussion

Many leukemia-causing gene rearrangements possess fusion breakpoints located within at least one fragile site, suggesting the potential for fragile site-mediated instability to play a role in leukemogenesis [10]. We found that a classic fragile-site inducing condition, low-dose APH, and two known fragile site-inducing chemicals, benzene, and DEN, generate significantly more DNA breaks at the BCRs of *MLL* and *CBFB*, compared to those in the untreated cells (Figs. 1 and 3). In addition to the chemicals that we used here, fragile sites are sensitive to a range of environmental and dietary agents, and chemotherapeutic drugs [5]. Therefore, our study points to the importance of investigating these chemicals and their role in inducing DNA breakage in leukemia-associated genes, and possibly in leading to disease-causing gene rearrangements. Many of these chemicals have demonstrated positive associations with the risk of leukemia, while some without a previous link to leukemia, such as DEN, appear to be worth investigating.

Stable DNA secondary structure is suggested to contribute to fragile site breakage. During DNA replication, fragile site-inducing conditions, such as low-dose APH, can cause an uncoupling of the helicase complex from the DNA polymerase, resulting in long stretches of single-stranded DNA. At fragile sites, this DNA can form stable DNA secondary structures that pause polymerase progression and result in DNA breakage [40,41]. Interestingly, the BCR of *MLL* possesses the potential to form stable secondary structures (Fig. 4). Fragile site breakage can also occur during transcription, resulting in collision of transcription and replication machinery and ultimately leading to DNA instability within these regions [42]. The difference in replication and transcription programs and overall gene expression patterns in different cell types appears to influence fragility in a cell type-specific manner

[43–46]. Although information about the direction of DNA replication along the *MLL* gene in CD34⁺ cells is not available, the *MLL* gene is highly expressed in CD34⁺ cells. Gene expression data from Su et al., indicates high levels of expression for *MLL*, *CBFB*, and *FHIT* in CD34⁺ cells relative to all tissue and cell types studied, while *RET* expression was slightly lower [47] (Supplemental Table 2). This may be related to our observation that overall breakages within *RET* occurred at a much lower level than at *MLL*, *CBFB*, or *FHIT* in HSPCs. It is unknown whether the chemicals investigated in this study influence the expression or chromatin organization of *MLL*, *CBFB*, or *FHIT* in CD34⁺ cells, but the reported high expression of these genes, as well as *TOP2A* and *TOP2B*, in these cells [47] is consistent with the model proposed for *MLL* rearrangement formation in which transcriptionally active genes are susceptible to topoisomerase II β -dependent breakage [35].

Topoisomerase II has critical functions in both DNA replication and transcription processes. The expression of topoisomerase II isoforms α and β are 10- and 7-fold higher in CD34⁺ cells, respectively, than the average for all tissues [47] (Supplemental Table 2). More recently, *MLL* rearrangement formation was proposed to involve topoisomerase II β -dependent DNA breakage in *MLL* and rearrangement partner genes *AF4* and *AF9* within shared transcription factories [35]. Our results similarly suggest a role for topoisomerase II in breakage at *MLL* and *CBFB*, as treatment with non-cytotoxic concentrations of etoposide and doxorubicin caused breakage at the BCRs of both leukemia-related genes. The 11-nt hotspot of chemical-induced cleavage that we found has been identified by several other studies as a strong topoisomerase II cleavage site [14,36,37]. These results, in combination with the strong association between chemical-induced breakpoints and predicted topoisomerase II cleavage sites in the *MLL* e12 and *CBFB* i5 regions (Table 1), further support a role for topoisomerase II-mediated breakage upon exposure to environmental agents.

The known mechanisms of action for the chemicals used in this study are diverse, yet the DNA breakage profiles at each region are strikingly similar. Aphidicolin is an inhibitor of DNA polymerases α , δ , and ϵ and is thought to cause breakage at fragile sites by exposing long stretches of single-stranded secondary structure-prone DNA that can lead to replication fork stall and collapse [48]. Aphidicolin was also recently shown to induce fragile site breakage through a topoisomerase II-mediated mechanism [3]. Benzene and DEN are carcinogenic environmental chemicals able to cause DNA adduct formation, while benzene metabolites hydroquinone and benzoquinone can inhibit topoisomerase II [39,49]. Etoposide and doxorubicin inhibit topoisomerase II by stabilizing cleavage complex formation and preventing DNA religation [50,51]. All chemicals used in our study, with the exception of DEN, are known to interact with topoisomerase II to cause DNA breakage. Our study suggests that a topoisomerase II-dependent mechanism is responsible for breakage within the BCRs of *MLL* and *CBFB*, and to our knowledge is the first to support a role for topoisomerase II in DEN-induced DNA breakage. Our data also suggests multiple determinants for such a topoisomerase II-dependent mechanism, in which the high number of potential topoisomerase cleavage sites provides the basis, and the associated DNA secondary structures and active transcription (perhaps collisions of replication and transcription machinery) are an added influence for the DNA breakage patterns observed in

the BCRs of *MLL* and *CBFB*. This fits into current working models explaining the mechanism for fragile site breakage in which differential gene expression and replication and transcription programs contribute to cell type-specific fragility [43–46]. However, further investigation into the interplay of these factors will be necessary to understand the generation of leukemia-causing gene rearrangements.

While others have shown the sensitivity of *MLL* to etoposide in various cell types [36,37], we demonstrated that even at approximately 100–1000-fold lower concentrations etoposide can still induce DNA breakage within *MLL* in primary HSPCs. At higher concentrations close to the levels of etoposide used in previous studies, we found that cell viability started to decline (Fig. 2A) and affected HSPC survival. The low concentrations of etoposide and doxorubicin may mimic the conditions of HSPCs that survive chemotherapeutic treatment but are still exposed to low levels of drugs, and thus, are prone to breakage at sites with the potential to form leukemia-causing gene rearrangements. Indeed, we found that DNA breakage following exposure of HSPCs to low concentrations of environmental chemicals or chemotherapeutic agents occurred at *MLL* and *CBFB*, which are involved in leukemia-causing gene rearrangements. Several studies have investigated the role of DNA repair in response to DNA damage in HSPCs and found that CD34⁺ HSPCs are more sensitive to damage than more committed progenitor cells [52,53]. These studies further suggest that HSPCs are prone to undergo apoptosis following exposure to ionizing radiation or DNA adduct-forming agents compared to mature cells. Our results indicate that although HSPCs are extremely sensitive to DNA damage, exposure to non-cytotoxic levels of environmental chemicals and chemotherapeutic agents can still induce DNA damage without causing cell death. In the context of secondary leukemia formation, HSPCs that are not killed by chemotherapy regimens could be exposed to low levels of drugs, leading to breakage at sites like *MLL* or *CBFB* with the potential to form leukemia-causing rearrangements. As the cells in our study remained viable and able to grow and divide following treatment, these DNA insults have the potential to perpetuate into daughter cells and lead to leukemogenesis.

5. Conclusions

Long-term exposure to environmental chemicals or chemotherapeutic agents, even at non-cytotoxic levels, can be detrimental to human health. The susceptibility of human HSPCs to DNA breakage at specific loci, such as within the BCRs of *MLL* and *CBFB*, has the potential to lead to formation of leukemia-causing gene rearrangements. The high frequency of topoisomerase II recognition sites in specific regions and the high expression of topoisomerase II in human CD34⁺ HSPCs present a favorable environment for breakage following exposure to agents targeting topoisomerase II activity. Further understanding of the mechanism for breakage at *MLL* and *CBFB* in HSPCs may provide a clearer path to prevention or treatment of leukemias with these rearrangements.

Supplementary Material

Refer to Web version on PubMed Central for supplementary material.

Acknowledgments

This work was supported by the NIH R01GM101192, and the study sponsors had no involvement in the study design; collection, analysis and interpretation of data; the writing of the manuscript; the decision to submit the manuscript for publication.

Abbreviations

HSPC	hematopoietic stem and progenitor cells
APH	aphidicolin
PBS	phosphate-buffered saline
DEN	diethylnitrosamine
BCR	breakpoint cluster region
LM-PCR	ligation-mediated PCR

References

1. Eastmond DA, Keshava N, Sonawane B. Lymphohematopoietic cancers induced by chemicals and other agents and their implications for risk evaluation: an overview. *Mutat Res.* 2014; 761:40–64.
2. Yunis JJ, Soreng AL, Bowe AE. Fragile sites are targets of diverse mutagens and carcinogens. *Oncogene.* 1987; 1:59–69. [PubMed: 3438083]
3. Dillon LW, Pierce LC, Lehman CE, Nikiforov YE, Wang YH. DNA topoisomerases participate in fragility of the oncogene RET. *PLoS One.* 2013; 8:e75741. [PubMed: 24040417]
4. Mrasek K, Schoder C, Teichmann AC, Behr K, Franze B, Wilhelm K, Blaurock N, Claussen U, Liehr T, Weise A. Global screening and extended nomenclature for 230 aphidicolin-inducible fragile sites, including 61 yet unreported ones. *Int J Oncol.* 2010; 36:929–940. [PubMed: 20198338]
5. Dillon LW, Lehman CE, Wang YH. The role of fragile sites in sporadic papillary thyroid carcinoma. *J Thyroid Res.* 2012; 2012:927683. [PubMed: 22762011]
6. Popescu NC. Genetic alterations in cancer as a result of breakage at fragile sites. *Cancer Lett.* 2003; 192:1–17. [PubMed: 12637148]
7. Arlt MF, Durkin SG, Ragland RL, Glover TW. Common fragile sites as targets for chromosome rearrangements. *DNA Repair.* 2006; 5:1126–1135. [PubMed: 16807141]
8. Durkin SG, Ragland RL, Arlt MF, Mulle JG, Warren ST, Glover TW. Replication stress induces tumor-like microdeletions in FHIT/FRA3B. *Proc Natl Acad Sci U S A.* 2008; 105:246–251. [PubMed: 18162546]
9. Gandhi M, Dillon LW, Pramanik S, Nikiforov YE, Wang YH. DNA breaks at fragile sites generate oncogenic RET/PTC rearrangements in human thyroid cells. *Oncogene.* 2010; 29:2272–2280. [PubMed: 20101222]
10. Burrow AA, Williams LE, Pierce LC, Wang YH. Over half of breakpoints in gene pairs involved in cancer-specific recurrent translocations are mapped to human chromosomal fragile sites. *BMC Genomics.* 2009; 10:59. [PubMed: 19183484]
11. Meyer C, Hofmann J, Burmeister T, Groger D, Park TS, Emerenciano M, Pombo de Oliveira M, Renneville A, Villarese P, Macintyre E, Cave H, Clappier E, Mass-Malo K, Zuna J, Trka J, De Braekeleer E, De Braekeleer M, Oh SH, Tsauro G, Fechina L, van der Velden VH, van Dongen JJ, Delabesse E, Binato R, Silva ML, Kustanovich A, Aleinikova O, Harris MH, Lund-Aho T, Juvonen V, Heidenreich O, Vormoor J, Choi WW, Jarosova M, Kolenova A, Bueno C, Menendez P, Wehr S, Eckert C, Talmant P, Tondeur S, Lippert E, Launay E, Henry C, Ballerini P, Lapillone H, Callanan MB, Cayuela JM, Herbaux C, Cazzaniga G, Kakadiya PM, Bohlander S, Ahlmann M, Choi JR, Gameiro P, Lee DS, Krauter J, Cornillet-Lefebvre P, Te Kronnie G, Schafer BW, Kubetzko S, Alonso CN, zur Stadt U, Sutton R, Venn NC, Izraeli S, Trakhtenbrot L, Madsen HO, Archer P, Hancock J, Cerveira N, Teixeira MR, Lo Nigro L, Moricke A, Stanulla M,

- Schrappé M, Sedek L, Szczepanski T, Zwaan CM, Coenen EA, van den Heuvel-Eibrink MM, Strehl S, Dworzak M, Panzer-Grumayer R, Dingermann T, Klingebiel T, Marschalek R. The MLL recombinome of acute leukemias in 2013. *Leukemia*. 2013; 27:2165–2176. [PubMed: 23628958]
12. Krivtsov AV, Armstrong SA. MLL translocations, histone modifications and leukaemia stem-cell development. *Nat Rev Cancer*. 2007; 7:823–833. [PubMed: 17957188]
 13. Khoury, H. The role of gene translocations in the molecular pathogenesis of acute myeloid leukemia. In: Leyden, GT., editor. *Genetic Translocations and Other Chromosome Aberrations*. Nova Science Publishers, Inc; New York: 2008. p. 1-47.
 14. Wright RL, Vaughan AT. A systematic description of MLL fusion gene formation. *Crit Rev Oncol Hematol*. 2014; 91:283–291. [PubMed: 24787275]
 15. Liu P, Tarle SA, Hajra A, Claxton DF, Marlton P, Freedman M, Siciliano MJ, Collins FS. Fusion between transcription factor CBF beta/PEBP2 beta and a myosin heavy chain in acute myeloid leukemia. *Science (New York, NY)*. 1993; 261:1041–1044.
 16. van der Reijden BA, Dauwerse HG, Giles RH, Jagmohan-Changur S, Wijmenga C, Liu PP, Smit B, Wessels HW, Beverstock GC, Jotterand-Bellomo M, Martinet D, Muhlematter D, Lafage-Pochitaloff M, Gabert J, Reiffers J, Bilhou-Nabera C, van Ommen GJ, Hagemeyer A, Breuning MH. Genomic acute myeloid leukemia-associated inv(16)(p13q22) breakpoints are tightly clustered. *Oncogene*. 1999; 18:543–550. [PubMed: 9927211]
 17. Chen W, Kumar AR, Hudson WA, Li Q, Wu B, Staggs RA, Lund EA, Sam TN, Kersey JH. Malignant transformation initiated by MLL-AF9: gene dosage and critical target cells. *Cancer Cell*. 2008; 13:432–440. [PubMed: 18455126]
 18. Krivtsov AV, Twomey D, Feng Z, Stubbs MC, Wang Y, Faber J, Levine JE, Wang J, Hahn WC, Gilliland DG, Golub TR, Armstrong SA. Transformation from committed progenitor to leukaemia stem cell initiated by MLL-AF9. *Nature*. 2006; 442:818–822. [PubMed: 16862118]
 19. Warner JK, Wang JC, Hope KJ, Jin L, Dick JE. Concepts of human leukemic development. *Oncogene*. 2004; 23:7164–7177. [PubMed: 15378077]
 20. Wei J, Wunderlich M, Fox C, Alvarez S, Cigudosa JC, Wilhelm JS, Zheng Y, Cancelas JA, Gu Y, Jansen M, Dimartino JF, Mulloy JC. Microenvironment determines lineage fate in a human model of MLL-AF9 leukemia. *Cancer Cell*. 2008; 13:483–495. [PubMed: 18538732]
 21. Jaiswal S, Weissman IL. Hematopoietic stem and progenitor cells and the inflammatory response. *Ann NY Acad Sci*. 2009; 1174:118–121. [PubMed: 19769744]
 22. Lévesque, JP.; Winkler, IG.; Larsen, SR.; Rasko, JEJ. Mobilization of bone marrow-derived progenitors. In: Kauser, K.; Zeiher, A-M., editors. *Bone Marrow-Derived Progenitors*. Vol. 180. Springer; Berlin Heidelberg: 2007. p. 3-36.
 23. Schulz C, von Andrian UH, Massberg S. Hematopoietic stem and progenitor cells: their mobilization and homing to bone marrow and peripheral tissue. *Immunol Res*. 2009; 44:160–168. [PubMed: 19340403]
 24. Zuker M. Mfold web server for nucleic acid folding and hybridization prediction. *Nucleic Acids Res*. 2003; 31:3406–3415. [PubMed: 12824337]
 25. Capranico G, Binaschi M. DNA sequence selectivity of topoisomerases and topoisomerase poisons. *Biochim Biophys Acta*. 1998; 1400:185–194. [PubMed: 9748568]
 26. Ju BG, Lunyak VV, Perissi V, Garcia-Bassets I, Rose DW, Glass CK, Rosenfeld MG. A topoisomerase IIbeta-mediated dsDNA break required for regulated transcription. *Science (New York, NY)*. 2006; 312:1798–1802.
 27. Froelich-Ammon SJ, Gale KC, Osheroff N. Site-specific cleavage of a DNA hairpin by topoisomerase II. DNA secondary structure as a determinant of enzyme recognition/cleavage. *J Biol Chem*. 1994; 269:7719–7725. [PubMed: 8125998]
 28. Jonstrup AT, Thomsen T, Wang Y, Knudsen BR, Koch J, Andersen AH. Hairpin structures formed by alpha satellite DNA of human centromeres are cleaved by human topoisomerase IIalpha. *Nucleic Acids Res*. 2008; 36:6165–6174. [PubMed: 18824478]
 29. Corbin S, Neilly ME, Espinosa R 3rd, Davis EM, McKeithan TW, Le Beau MM. Identification of unstable sequences within the common fragile site at 3p14. 2: implications for the mechanism of deletions within fragile histidine triad gene/common fragile site at 3p14. 2 in tumors. *Cancer Res*. 2002; 62:3477–3484. [PubMed: 12067991]

30. Zlotorynski E, Rahat A, Skaug J, Ben-Porat N, Ozeri E, Hershberg R, Levi A, Scherer SW, Margalit H, Kerem B. Molecular basis for expression of common and rare fragile sites. *Mol Cell Biol.* 2003; 23:7143–7151. [PubMed: 14517285]
31. Smanik PA, Furminger TL, Mazzaferri EL, Jhiang SM. Breakpoint characterization of the ret/PTC oncogene in human papillary thyroid carcinoma. *Hum Mol Genet.* 1995; 4:2313–2318. [PubMed: 8634704]
32. Dillon LW, Burrow AA, Wang YH. DNA instability at chromosomal fragile sites in cancer. *Curr Genomics.* 2010; 11:326–337. [PubMed: 21286310]
33. Kontny NE, Wurthwein G, Joachim B, Boddy AV, Krischke M, Fuhr U, Thompson PA, Jorger M, Schellens JH, Hempel G. Population pharmacokinetics of doxorubicin: establishment of a NONMEM model for adults and children older than 3 years. *Cancer Chemother Pharmacol.* 2013; 71:749–763. [PubMed: 23314734]
34. Kersting G, Willmann S, Wurthwein G, Lippert J, Boos J, Hempel G. Physiologically based pharmacokinetic modelling of high- and low-dose etoposide: from adults to children. *Cancer Chemother Pharmacol.* 2012; 69:397–405. [PubMed: 21789689]
35. Cowell IG, Sondka Z, Smith K, Lee KC, Manville CM, Sidorczuk-Lesthuruge M, Rance HA, Padgett K, Jackson GH, Adachi N, Austin CA. Model for MLL translocations in therapy-related leukemia involving topoisomerase II β -mediated DNA strand breaks and gene proximity. *Proc Natl Acad Sci U S A.* 2012; 109:8989–8994. [PubMed: 22615413]
36. Le H, Singh S, Shih SJ, Du N, Schnyder S, Loreda GA, Bien C, Michaelis L, Toor A, Diaz MO, Vaughan AT. Rearrangements of the MLL gene are influenced by DNA secondary structure, potentially mediated by topoisomerase II binding. *Genes Chromosomes Cancer.* 2009; 48:806–815. [PubMed: 19530238]
37. Scharf S, Zech J, Bursen A, Schraets D, Oliver PL, Kliem S, Pfitzner E, Gillert E, Dingermann T, Marschalek R. Transcription linked to recombination: a gene-internal promoter coincides with the recombination hot spot II of the human MLL gene. *Oncogene.* 2007; 26:1361–1371. [PubMed: 16983345]
38. Dillon LW, Pierce LC, Ng MC, Wang YH. Role of DNA secondary structures in fragile site breakage along human chromosome 10. *Hum Mol Genet.* 2013; 22:1443–1456. [PubMed: 23297364]
39. Lindsey RH Jr, Bromberg KD, Felix CA, Osheroff N. 1,4-Benzoquinone is a topoisomerase II poison. *Biochemistry.* 2004; 43:7563–7574. [PubMed: 15182198]
40. Burrow AA, Marullo A, Holder LR, Wang YH. Secondary structure formation and DNA instability at fragile site FRA16B. *Nucleic Acids Res.* 2010; 38:2865–2877. [PubMed: 20071743]
41. Zhang H, Freudenreich CH. An AT-rich sequence in human common fragile site FRA16D causes fork stalling and chromosome breakage in *S. cerevisiae*. *Mol Cell.* 2007; 27:367–379. [PubMed: 17679088]
42. Helmrich A, Ballarino M, Tora L. Collisions between replication and transcription complexes cause common fragile site instability at the longest human genes. *Mol Cell.* 2011; 44:966–977. [PubMed: 22195969]
43. Debatisse M, Le Tallec B, Letessier A, Dutrillaux B, Brison O. Common fragile sites: mechanisms of instability revisited. *Trends Genet.* 2012; 28:22–32. [PubMed: 22094264]
44. Le Tallec B, Dutrillaux B, Lachages AM, Millot GA, Brison O, Debatisse M. Molecular profiling of common fragile sites in human fibroblasts. *Nat Struct Mol Biol.* 2011; 18:1421–1423. [PubMed: 22056772]
45. Letessier A, Millot GA, Koundrioukoff S, Lachages AM, Vogt N, Hansen RS, Malfoy B, Brison O, Debatisse M. Cell-type-specific replication initiation programs set fragility of the FRA3B fragile site. *Nature.* 2011; 470:120–123. [PubMed: 21258320]
46. Re A, Cora D, Puliti AM, Caselle M, Sbrana I. Correlated fragile site expression allows the identification of candidate fragile genes involved in immunity and associated with carcinogenesis. *BMC Bioinf.* 2006; 7:413.
47. Su AI, Wiltshire T, Batalov S, Lapp H, Ching KA, Block D, Zhang J, Soden R, Hayakawa M, Kreiman G, Cooke MP, Walker JR, Hogenesch JB. A gene atlas of the mouse and human protein-encoding transcriptomes. *Proc Natl Acad Sci U S A.* 2004; 101:6062–6067. [PubMed: 15075390]

48. Durkin SG, Glover TW. Chromosome fragile sites. *Annu Rev Genet.* 2007; 41:169–192. [PubMed: 17608616]
49. Lindsey RH, Bender RP, Osheroff N. Stimulation of topoisomerase II-mediated DNA cleavage by benzene metabolites. *Chem Biol Interact.* 2005; 153–154:197–205.
50. Osheroff N. Effect of antineoplastic agents on the DNA cleavage/religation reaction of eukaryotic topoisomerase II: inhibition of DNA religation by etoposide. *Biochemistry.* 1989; 28:6157–6160. [PubMed: 2551366]
51. Bodley A, Liu LF, Israel M, Seshadri R, Koseki Y, Giuliani FC, Kirschenbaum S, Silber R, Potmesil M. DNA topoisomerase II-mediated interaction of doxorubicin and daunorubicin congeners with DNA. *Cancer Res.* 1989; 49:5969–5978. [PubMed: 2551497]
52. Milyavsky M, Gan OI, Trottier M, Komosa M, Tabach O, Notta F, Lechman E, Hermans KG, Eppert K, Konovalova Z, Ornatsky O, Domany E, Meyn MS, Dick JE. A distinctive DNA damage response in human hematopoietic stem cells reveals an apoptosis-independent role for p53 in self-renewal. *Cell Stem Cell.* 2010; 7:186–197. [PubMed: 20619763]
53. Bracker TU, Giebel B, Spanholtz J, Sorg UR, Klein-Hitpass L, Moritz T, Thomale J. Stringent regulation of DNA repair during human hematopoietic differentiation: a gene expression and functional analysis. *Stem Cells.* 2006; 24:722–730. [PubMed: 16195417]

Appendix A. Supplementary data

Supplementary data associated with this article can be found, in the online version, at <http://dx.doi.org/10.1016/j.mrfmmm.2015.06.011>

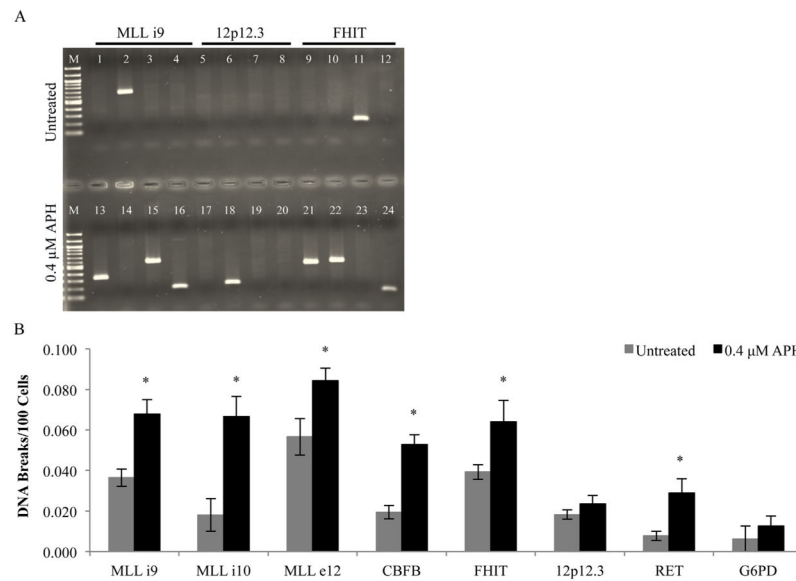


Fig. 1. LM-PCR detection of DNA breaks generated in human CD34⁺ cells after treatment with APH. (A) DNA breaks formed in intron 9 of *MLL*, the non-fragile 12p12.3 region, and intron 4 of *FHIT* were detected by LM-PCR. A representative gel is shown. Lanes 1–12 represent breaks in DNA from untreated cells, lanes 13–24 represent breaks detected in DNA from cells treated with APH. Each lane represents a separate PCR reaction using DNA from approximately 1300 cells. The M lane is a 100 bp molecular weight ladder, and bands below 100 bp correspond to primer dimers. (B) The frequency of DNA breakage in untreated cells, or cells treated with APH in the regions depicted in (A) as well as intron 10 and exon 12 of *MLL*, intron 5 of *CBFB*, and intron 11 of *RET*. The breakage frequency is presented as DNA breaks per 100 cells, and is the average of at least 3 experimental replicates with error bars representing standard errors. Asterisks mark $p < 0.05$ as compared to the respective untreated samples.

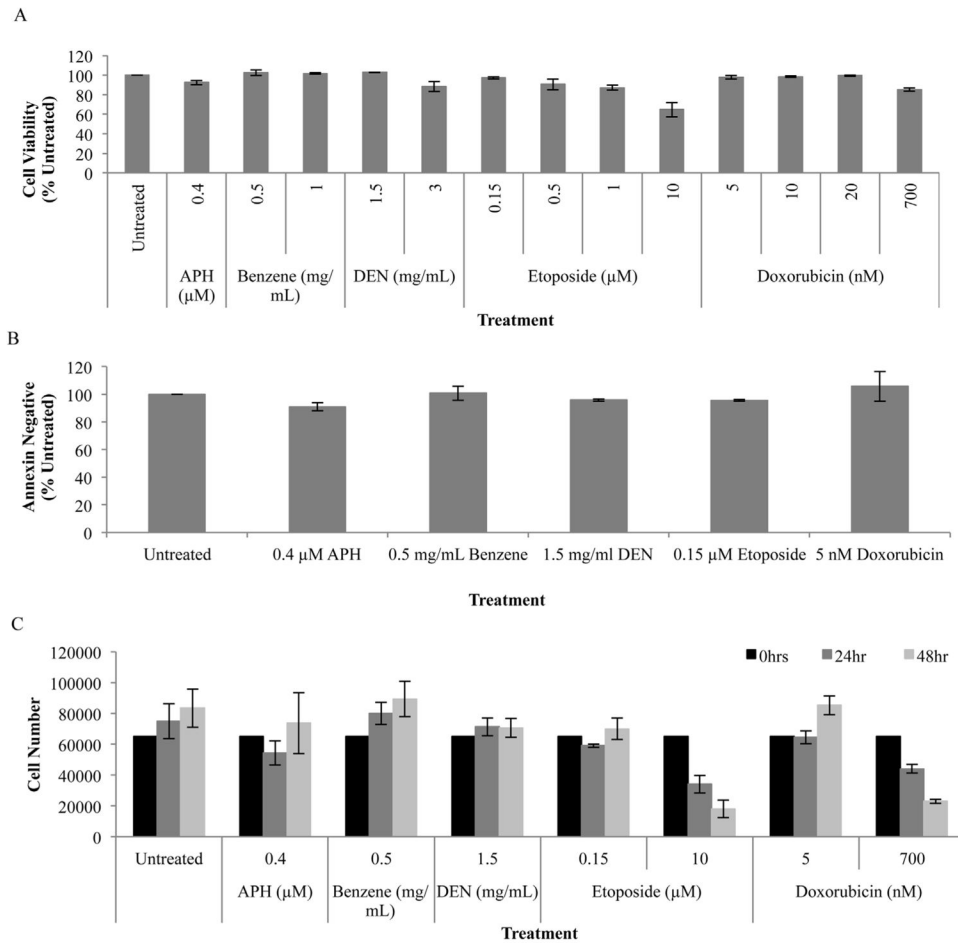


Fig. 2. Characterization of human CD34⁺ cell survival, and growth, following treatment with APH, benzene, DEN, etoposide, and doxorubicin. (A) Cell viability was determined by propidium-iodide stain, and measured using flow cytometry, after treatment with various concentrations of chemicals. (B) The number of cells undergoing active apoptosis following treatment with chemicals was determined using Annexin V stain and measured by flow cytometry. (C) The level of cell growth following treatment was determined by quantification using a hemocytometer. Cells were counted at the time of plating (0 h), after 24 h treatment (24 h), or allowed to recover for an additional 24 h after chemicals had been removed (48 h). Data (A–C) is represented by the average of at least 3 replicates with error bars representing standard deviations.

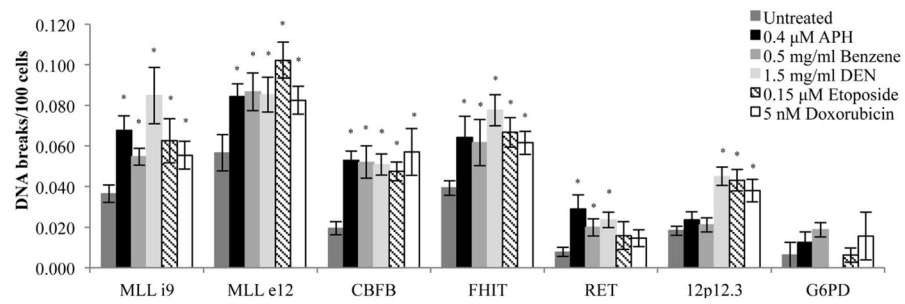


Fig. 3. The frequency of DNA breakage in human CD34⁺ cells after 24 h treatments with fragile site-inducing chemicals or chemotherapeutic drugs at the MLL i9, MLL e12, CBFB i5, FHIT, RET, 12p12.3, and G6PD regions. The breakage frequency is given as DNA breaks per 100 cells, and is the average of at least 3 replicates with error bars representing standard errors. Asterisks mark $p < 0.05$ as compared to the respective untreated samples.

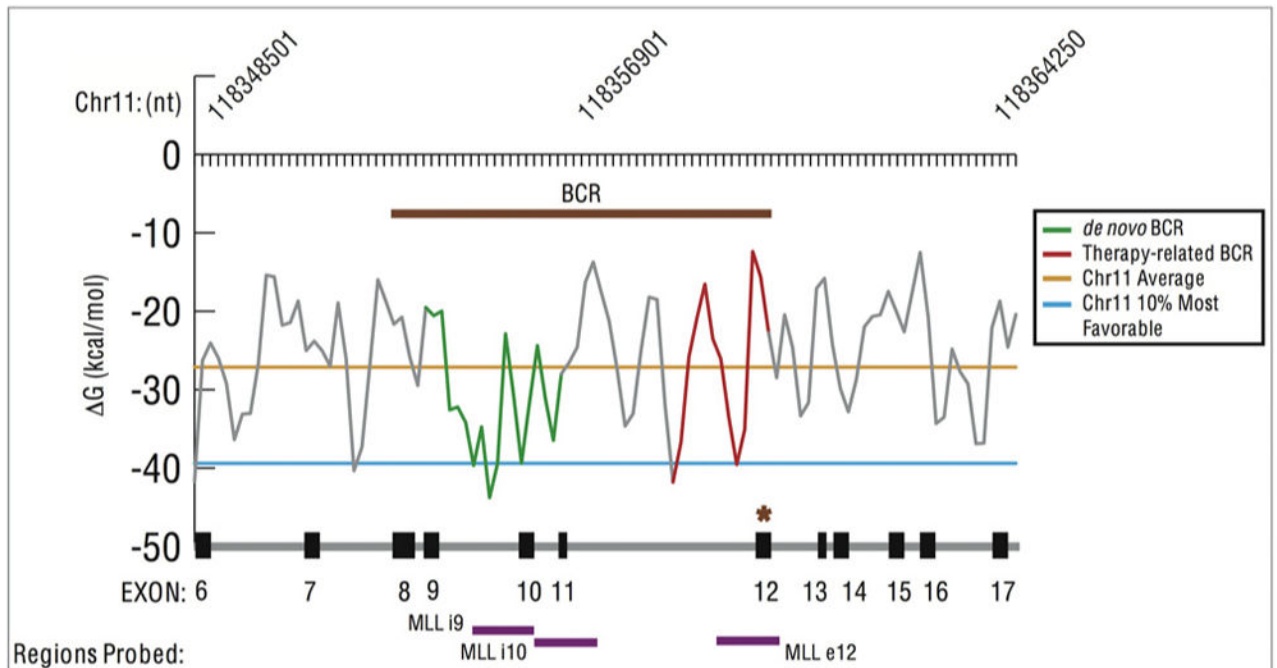


Fig. 4.

DNA secondary structure prediction within the patient BCRs of *MLL*. The computed lowest free-energy values for the predicted secondary structure from 300-nt segments analyzed by the Mfold program, were compared to the average free energy of chromosome 11 (-27.1 kcal/mol, horizontal orange line) or the most favorable 10% of free energy values on chromosome 11 (-39.4 kcal/mol, horizontal blue line). The *x*-axis indicates the *MLL* region, and the *y*-axis displays the free energy of the predicted structure. The BCR of *MLL* (exons 8 to 12, chr11: 118352430-118359475, brown bar) contain a *de novo* BCR (green line), and a therapy-related cluster region (red line) [11,14]. The brown star represents the topoisomerase II cleavage hotspot [36,37]. The purple bars designate the regions analyzed by LM-PCR: MLL i9, chr11: 118353926-118354976; MLL i10, chr11: 118355148-118356198; MLL e12, chr11: 118358609-118359659. (For interpretation of the references to color in this figure legend, the reader is referred to the web version of this article.)

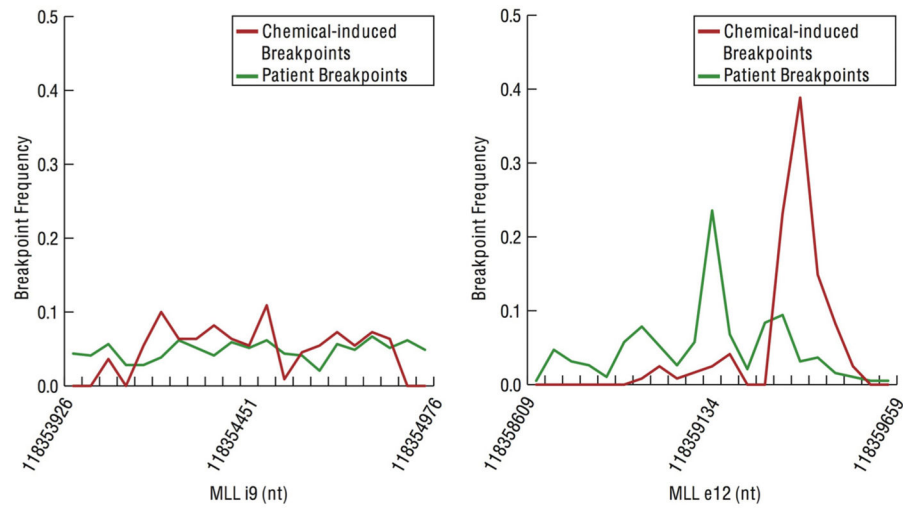


Fig. 5. Distribution of chemical-induced and patient breakpoints within the MLL i9 and MLL e12 regions. The location of leukemia patient breakpoints [11] and the location of chemical-induced breakpoints from our study were placed into 50-bp bins corresponding to the (A) MLL i9 region (389 patient breakpoints vs. 110 chemical-induced breakpoints) or (B) MLL e12 region (191 patient breakpoints vs. 120 chemical-induced breakpoints). The breakpoint frequency is presented as a percentage of breakpoints located within each 50-bp bin relative to the total breakpoints in the respective 1050-bp region.

Table 1

Frequency of chemical-induced DNA breakpoints located at predicted topoisomerase II cleavage sites.

	Number of breaks at topo II cleavage sites ^a	Total number of breaks mapped	% of breaks at topo II sites	Breaks at topo II sites/100 cells ± SE (<i>p</i> values relative to the respective untreated) ^b
MLL i9				
Untreated	23	25	92	0.034 ± 0.004
APH	16	21	76	0.052 ± 0.005 (0.010)
Benzene	18	23	78	0.043 ± 0.003 (0.102)
DEN	18	28	64	0.054 ± 0.009 (0.027)
Etoposide	15	17	88	0.055 ± 0.010 (0.024)
Doxorubicin	19	21	90	0.050 ± 0.006 (0.022)
Total	109	135	81	
MLL e12				
Untreated	18	21	86	0.049 ± 0.008
APH	22	25	88	0.074 ± 0.006 (0.011)
Benzene	26	27	96	0.083 ± 0.009 (0.006)
DEN	28	29	97	0.083 ± 0.008 (0.008)
Etoposide	18	19	95	0.097 ± 0.008 (<0.001)
Doxorubicin	18	20	90	0.074 ± 0.006 (0.018)
Total	130	141	92	
CBFB i5				
Untreated	12	18	67	0.013 ± 0.002
APH	20	21	95	0.050 ± 0.004 (<0.001)
Benzene	18	19	95	0.050 ± 0.008 (<0.001)
DEN	18	20	90	0.046 ± 0.005 (<0.001)
Etoposide	19	19	100	0.048 ± 0.005 (<0.001)
Doxorubicin	15	18	83	0.039 ± 0.012 (<0.001)
Total	102	115	89	

^aTopoisomerase cleavage sites determined by DNA secondary structures (one nucleotide from the junction of the 3'-base of a hairpin stem with single-stranded DNA, and within the single-stranded DNA loop of the hairpin structure [27,28]), or consensus sequences: [5'-(no A) (no T) (A/no C) (-) (C/no A) (-) (-) (-) (-) (no T) (-) (T/no G) (C/no A) (-)-3'], where breakage occurs between nucleotides five and six [25], and the consensus sequence [5'-(A) (T) (T) (A/T)- 3'], where the breakage occurs before the first nucleotide [26].

^b*p*-Values were calculated using two-tailed Student's *t*-tests.